Radiation-produced defects in germanium: experimental data and models of defects

© V.V. Emtsev[1], V.V. Kozlovski[2], D.S. Poloskin[1], G.A. Oganesyan[1]

[1] Ioffe Institute,
194021 St. Petersburg, Russia
[2] Peter the Great St.Petersburg Polytechnic University,
195251 St. Petersburg, Russia

E-mail: emtsev@mail.ioffe.ru

(Received 3.04.2017. Received after revision 15.06.2017)

The problem of radiation-produced defects in *n*-Ge before and after $n \to p$ conversion is discussed in the light of electrical data obtained by means of Hall effect measurements as well as Deep Level Transient Spectroscopy. The picture of the dominant radiation defects in irradiated *n*-Ge before $n \to p$ conversion appears to be complicated, since they turn out to be neutral in *n*-type material and unobserved in the electrical measurements. It is argued that radiation-produced acceptors at $\approx E_C - 0.2$ eV previously ascribed to vacancy-donor pairs (*E*-centers) play a minor role in the defect formation processes under irradiation. Acceptor defects at $\approx E_V + 0.1$ eV are absolutely dominating in irradiated *n*-Ge after $n \to p$ conversion. All the radiation defects under consideration were found to be dependent on the chemical group-*V* impurities. Together with this, they are concluded to be vacancy-related, as evidenced positron annihilation experiments. A detailed consideration of experimental data on irradiated *n*-Ge shows that the present model of radiation-produced defects adopted in literature should be reconsidered.

DOI: 10.21883/FTP.2017.12.45178.8599

1. Introduction

In recent years great progress has been achieved in solving many problems associated with germanium technology and processing. This, in turn, has provided impetus for a better understanding the fundamental physical properties of impurities and other structural defects in Ge and how to use them in various electronic devices [1]. Our knowledge has been supplemented by extensive theoretical studies of point defects, including *ab-initio* modeling; see Chapt. 6 in [1] and below in Section 3. It is well-known that a vast amount of information on defect properties and behavior comes from radiation experiments on semiconductors. Radiation-produced defects in silicon have been cited as an excellent example of this kind; see for instance review [2].

In sharp contrast to Si, the identification of defects in irradiated Ge is still poor, because Electronic Paramagnetic Resonance (EPR) and related atomic−structure sensitive techniques appear to have been less successful in this semiconductor. Electrical and optical measurements, among them Hall effect, Deep Level Transient Spectroscopy (DLTS), including Laplace DLTS (LDLTS), Infrared Spectroscopy (IR Spectroscopy) etc., have allowed one to gain a lot of experimental data on Ge concerning properties of impurity−related complexes with intrinsic point defects. Many hundreds of such experiments on irradiated Ge have been carried out over many decades, in parallel to the more extensive studies of irradiated Si. The present paper is aimed at highlighting some challenging points in the identification of radiation−produced defects in Ge, but not at giving a survey of all of the experimental and theoretical information gained so far. In the lack of reliable data on atomic structures of impurity−related complexes in Ge a general way of theoretical modeling of structural defects is to look at what is known to be going on in irradiated Si, based on many similarities of the behavior of impurities in the both semiconductors. However, one should keep in mind that this way may be sometimes misleading, especially looking at the energy spectra of defects. To cite some simple examples, mentioned should be the energy spectra the of substitutional acceptor impurities B and In as well the donor impurities P and Bi in Si as compared to those in Ge. Another excellent example of this kind can be the well−known fact that the behavior of *p*-Si and *p*-Ge doped with shallow group-III acceptors is rather different under fast electron irradiation. Actually, *p*-Si materials can be easily damaged while the resistance of *p*-Ge to radiation damage is known to be much higher; see Item 2.6, below. To our opinion, it is time to outline some important findings in this field in order to discuss critical points of defect studies in Ge, separating what is reliably established from what is believed or claimed. The behavior of oxygen-lean *n*-Ge subjected to fast electron irradiation at room temperature, including $n \to p$ conversion of conductivity, will be our initial concern, because it makes possible understanding the key features of defect formation as compared to those known for irradiated floating−zone *n*-Si; see for instance [2]. To simplify this consideration, we limit ourselves for a major part to electron irradiation conditions at a few MeV or ^{60}Co gamma-rays when the role of intrinsic point defects like single vacancies and self-interstitials in defect interactions with impurity atoms is of primary importance. (It will be remembered that irradiation of Ge with ^{60}Co gamma-rays is equivalent to internal irradiation of samples with electrons at averaged energy of 660 keV due to Compton scattering of gamma-photons). Theoretical simulations will also be briefly discussed in comparison to the experimental data

considered. In conclusion some critical points in studies of radiation–produced defects in Ge will be presented.

2. Radiation-produced defects in Ge doped with group-*V* impurities

In what follows we are going to discuss some significant findings obtained with the help of Hall effect measurements on irradiated *n*-Ge. These results will be amplified by data furnished by means of DLTS and positron annihilation spectroscopy. The aim is to get a generalized picture of the dominant radiation defects formed before and after $n \to p$ conversion of conductivity. The oxygen concentration in the *n*-Ge doped with P, As, Sb, and Bi was a few $10^{15}\,\mathrm{cm}^{-3}$, so the role of oxygen-related defects should be subsidiary. Some of the wafers of *n*-Ge doped with Bi, however, had higher oxygen content, about $8 \cdot 10^{15}\,\mathrm{cm}^{-3}$ and in this case a contribution of oxygen-related complexes could be traced by Hall effect measurements; see Item 2.10, below.

2.1. Kinetics of defect formation in irradiated *n*-Ge before $n \to p$ conversion

Owing to the relative simplicity of Hall effect measurements taken over a temperature range of 78 to 300 K there is a lot of Hall effect data on irradiated *n*-Ge in literature. A typical example of such curves $n(1/T)$ for the oxygen-lean *n*-Ge doped with P is shown in Fig. 1 where the electron concentration n in the conduction band is displayed as

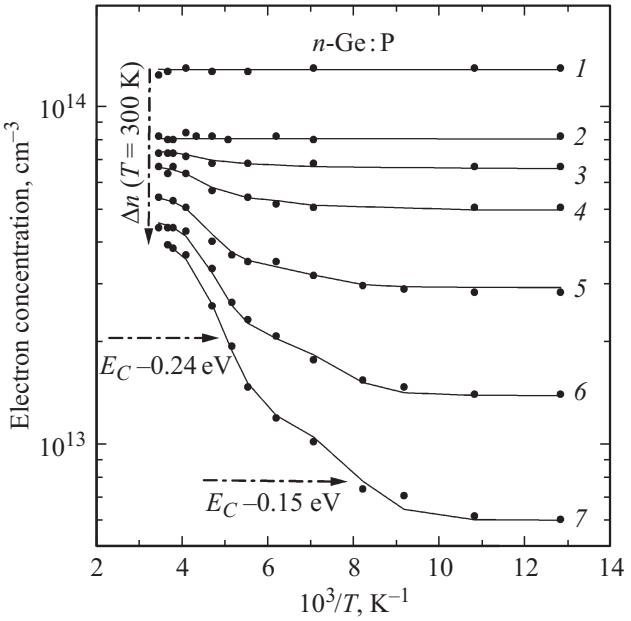

Figure 1. Electron concentration *vs* reciprocal temperature for the *n*-Ge : P before and after gamma-irradiation. Points, experimental; curves, calculated. Curve *1*, initial; curves *2*–*7*, irradiated. Dose Φ, $\times 10^{16}\,\mathrm{cm}^{-2}$: *1* — 0, *2* — 2.2, *3* — 3.4, *4* — 4.7, *5* — 6.1, *6* — 7.3, *7* — 8.1. Ionization energies of radiation-produced defects are given.

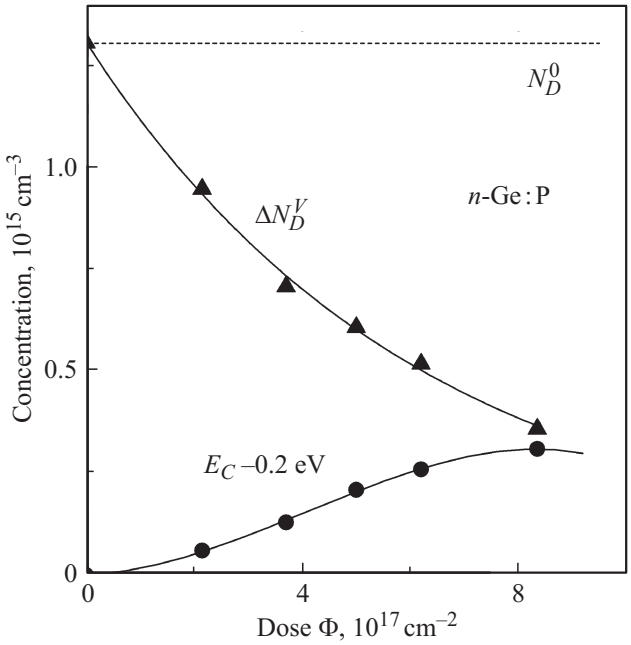

Figure 2. Dose dependence of radiation-produced defects in the *n*-Ge : P irradiated with gamma-rays. Changes in concentration of shallow donor states ΔN_D^V being equal to the concentrations of electrically neutral defects in the irradiated sample are defined as Δn ($T = 300\,\mathrm{K}$). N_D^0 shows the initial concentration of group-*V* impurity.

a function of reciprocal temperature. Two processes of radiation defect formation leading to a substantial decrease in the electron concentration are evident. First, the electron concentration at room temperature is markedly decreased by $2.5 \cdot 10^{13}\,\mathrm{cm}^{-3}$ just at the beginning of irradiation, at a dose of $\Phi = 2.2 \cdot 10^{16}\,\mathrm{cm}^{-2}$, but no defects with energy states in the upper half of the band gap are formed in noticeable concentration, at least in concentration larger than $1 \cdot 10^{13}\,\mathrm{cm}^{-3}$. This effect was earlier interpreted as the formation of deep radiation-produced acceptors whose concentration N_A^{rad} was believed to be equal to the difference between the electron concentrations at room temperature in *n*-Ge before and after irradiation, $\Delta n = n(\Phi = 0) - n(\Phi)$ where $n(\Phi = 0)$ and $n(\Phi)$ are the charge carrier concentrations at $T = 300\,\mathrm{K}$ in the initial state and after irradiation at dose Φ. Thus, this explanation suggested a simple compensation of electron conductivity by deep acceptors. Second, radiation defects at $\approx E_C - 0.2\,\mathrm{eV}$ make their appearance gradually with increasing dose; see Fig. 1. The latter defects were often claimed to be acceptors in the past, without reliable arguments. As is seen, their concentration $N_{0.2}^{\mathrm{rad}}$ appears to be substantially less than Δn ($T = 300\,\mathrm{K}$). Similar kinetics have also been reported for oxygen-lean *n*-Ge doped with As, Sb, and Bi, always with the delayed formation of defects at $\approx E_C - 0.2\,\mathrm{eV}$; see also [3–5]. For illustration purposes two of them are reproduced in Figs 2 and 3. It has been observed that together with the formation of the dominant defects, irradiation of *n*-Ge also results in the formation of other defects in small concentration; see

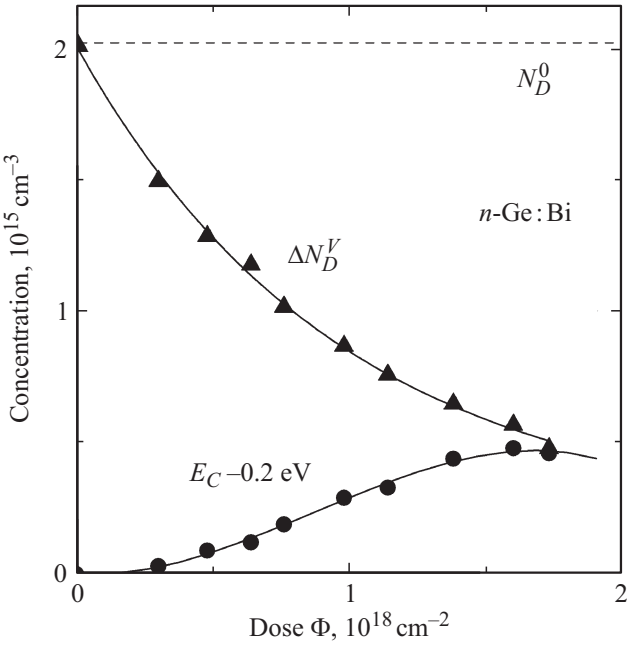

Figure 3. Dose dependence of radiation-produced defects in the n-Ge : Bi irradiated with gamma-rays. Changes in concentration of shallow donor states ΔN_D^V being equal to the concentration of electrically neutral defects in the irradiated sample are defined as Δn ($T = 300$ K). N_D^0 shows the initial concentration of group-V impurity.

Fig. 1. In what follows we pay attention primarily to the dominant radiation-produced defects.

Because the role of group-V impurities in the formation of impurity-related defects had been established by EPR for oxygen-lean n-Si, the question of similar reactions between shallow donors and intrinsic point defects in n-Ge was also considered. This question was explored by means of Hall effect measurements on irradiated n-Ge at cryogenic temperatures down to $T \approx 8$ K where ionization of shallow donors takes place.

2.2. Low-temperature Hall effect measurements on irradiated n-Ge before $n \to p$ conversion

Owing to the importance of this issue let's discuss it in some detail. Fig. 4, a–c displays two curves of $n(1/T)$ for the initial and irradiated n-Ge doped with P. These curves can be analyzed by means of relevant equations of charge balance [3,6]. In this way one can determine the total concentration of shallow donors N_D^V as well as the total concentration of compensating acceptors N_A. It should be noted that N_D^V includes all shallow donor states of group-V impurity independent of whether they are filled with electrons or empty of electrons due to compensation by acceptors at $T = 0$ K. Correspondently, N_A includes all compensating acceptor states in the band gap, because the Fermi level is placed close to the shallow donor states over a temperature range where the shallow donors start to be ionized. In the case of non-degenerate n-Ge one can calculate $n(1/T)$ curves making use of the following equation

$$\frac{n(n+N_A)}{N_D^V - N_A - n} = N_C T^{3/2} \frac{\exp(-\frac{E_D}{kT})}{2 + 6\exp(-\frac{\delta}{kT})}$$

where N_C is the effective density-of-states of the conduction band, E_D is the ionization energy of the singlet ground states, δ is the splitting between the singlet and triplet ground states of shallow donors, taken from optical measurements; other symbols have their usual meanings. Such an analysis allows one to see what happens with the shallow donors in irradiated n-Ge. If they interact with mobile intrinsic point defects produced during irradiation, as has been established in irradiated n-Si, the total concentration N_D^V must be decreased after irradiation. Concurrently, it is of keen interest to estallished what happens with the total concentration of compensating acceptors N_A as a result of irradiation. An analysis of the $n(1/T)$ curves recorded on oxygen-lean n-Ge doped with P, As, Sb, and Bi permits one to draw some important conclusions. First of all, there is ample evidence that group-V impurity atoms do strongly interact with intrinsic point defects. As a consequence, a marked loss of shallow donor states $\Delta N_D^V(\Phi) = N_D^V(\Phi) - N_D^V(\Phi = 0) = -7.28 \cdot 10^{13}$ cm^{-3} in the irradiated n-Ge is observed, where $N_D^V(\Phi = 0)$ is the initial concentration of shallow donors; see Fig. 4, a. In addition, the total concentration of all acceptors $N_A(\Phi)$ is growing with increasing dose Φ, the increase in N_A being close to the concentration $N_{0.2}^{\text{rad}}$ of the radiation-produced defects at $\approx E_C - 0.2$ eV. For example, $\Delta N_A(\Phi) = N_A(\Phi) - N_A(\Phi = 0) = +3.02 \cdot 10^{13}$ cm$^{-3} \approx N_{0.2}^{\text{rad}}$, where $N_A(\Phi = 0)$ is the total concentration of acceptors in the n-Ge before irradiation. Actually, it should be noted that $\Delta N_A(\Phi)$ is nearly equal also to the sum of the concentrations of defects at $\approx E_C - 0.22$ eV and $\approx E_C - 0.16$ eV. In other words, this points to the fact that these radiation defects are of acceptor type. The radiation-produced acceptors at $\approx E_C - 0.2$ eV appear to be dominant among the other electrically active defects. In the equation of charge balance all acceptors are assumed to be single. The long-standing question of whether defects at $\approx E_C - 0.2$ eV may be double acceptors seems not to be supported by Hall effect data, since the calculated curve in this case falls beyond all the experimental points due to the increasing compensation ratio at low cryogenic temperatures; see Fig. 4, b. The results obtained on irradiated n-Ge with higher concentration of shallow donors [3] provided additional support to this conclusion. In moderately doped n-Ge the radiation-produced acceptors under consideration are mostly free of electrons at room temperature and, therefore, the loss of shallow donor states $-\Delta N_D^V$ in irradiated oxygen-lean n-Ge is well characterized by Δn ($T = 300$ K); see Fig. 1 and 4, c. Furthermore, it is particularly remarkable that the loss of shallow donor states in irradiated n-Ge turned out to be larger by several times than the concentration of radiation acceptors $|-\Delta N_D^V| \gg \Delta N_A$. This may happen

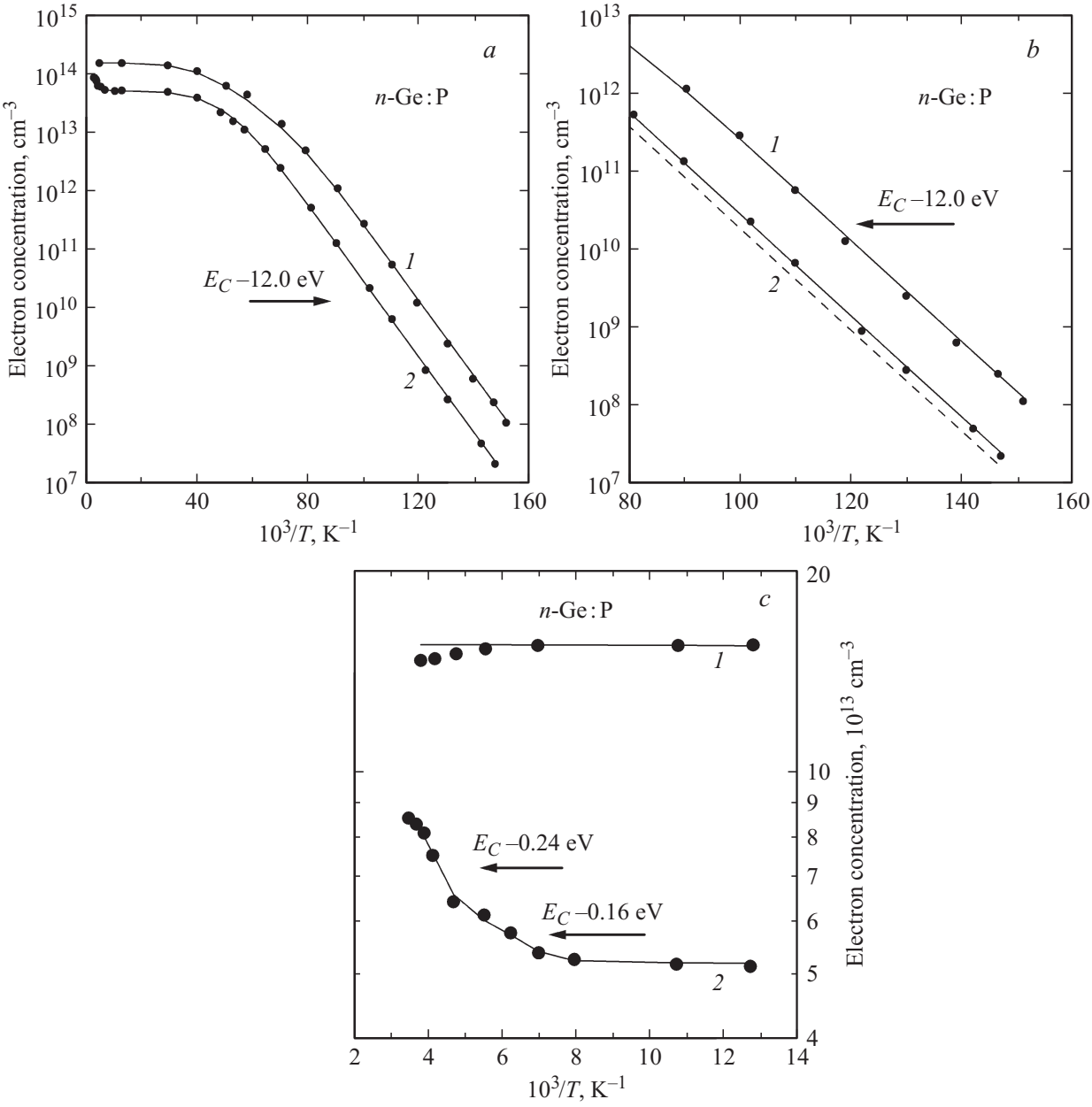

Figure 4. *a* — electron concentration *vs* reciprocal temperature for the *n*-Ge : P before and after gamma-irradiation. Points, experimental; curves, calculated. Curve *1*, initial; curve *2*, irradiated. Dose Φ, cm^{-2}; $5.4 \cdot 10^{16}$. Initial parameters: $E_D = 12.0$ meV; $\delta = 2.83$ meV; $N_D^V = 1.71 \cdot 10^{14}$ cm^{-3}; $N_A = 1.6 \cdot 10^{13}$ cm^{-3}. Parameters after the irradiation: $E_D = 12.0$ meV; $\delta = 2.83$ meV; $N_D^V = 9.82 \cdot 10^{13}$ cm^{-3}; $N_A = 4.62 \cdot 10^{13}$ cm^{-3}. Concentrations of single acceptor radiation-produced defects in the irradiated sample: $N_{0.16}^{\text{rad}} = 7 \cdot 10^{12}$ cm^{-3} ($E_C - 0.16$ eV); $N_{0.2}^{\text{rad}} = 2.7 \cdot 10^{13}$ cm^{-3} ($\approx E_C - 0.24$ eV). The ionization energies of the latter defects are accurate to 10 percent. *b* — electron concentration *vs* reciprocal temperature for the *n*-Ge : P before and after gamma-irradiation displayed on the expanded scale. Points, experimental; curves, calculated. Curve *1*, initial; curve *2*, irradiated. Dose Φ, cm^{-2}: $5.4 \cdot 10^{16}$. The parameters of the solid calculated lines are the same as in Fig. 1. If radiation defects at $\approx E_C - 0.24$ eV could be double acceptors also having deep acceptor states the dashed line shows the difference. *c* — electron concentration *vs* reciprocal temperature for the *n*-Ge : P before and after gamma-irradiation displayed on the expanded scale. Points, experimental; curves, calculated. Curve *1*, initial; curve *2*, irradiated. Dose Φ, cm^{-2}: $5.4 \cdot 10^{16}$. The parameters of the calculated lines are the same as in (*a*).

if the dominant impurity-related defects are electrically neutral in *n*-type Ge, say, having deep donor states in the band gap. Similar effects have also been observed in *n*-Ge : P and Ge:Bi irradiated with fast electrons at 0.9 MeV [7].

2.3. On the nature of dominant radiation defects in irradiated *n*-Ge before $n \to p$ conversion

The next question one is faced with, therefore, is what kind of impurity-related defects are formed in irradiated

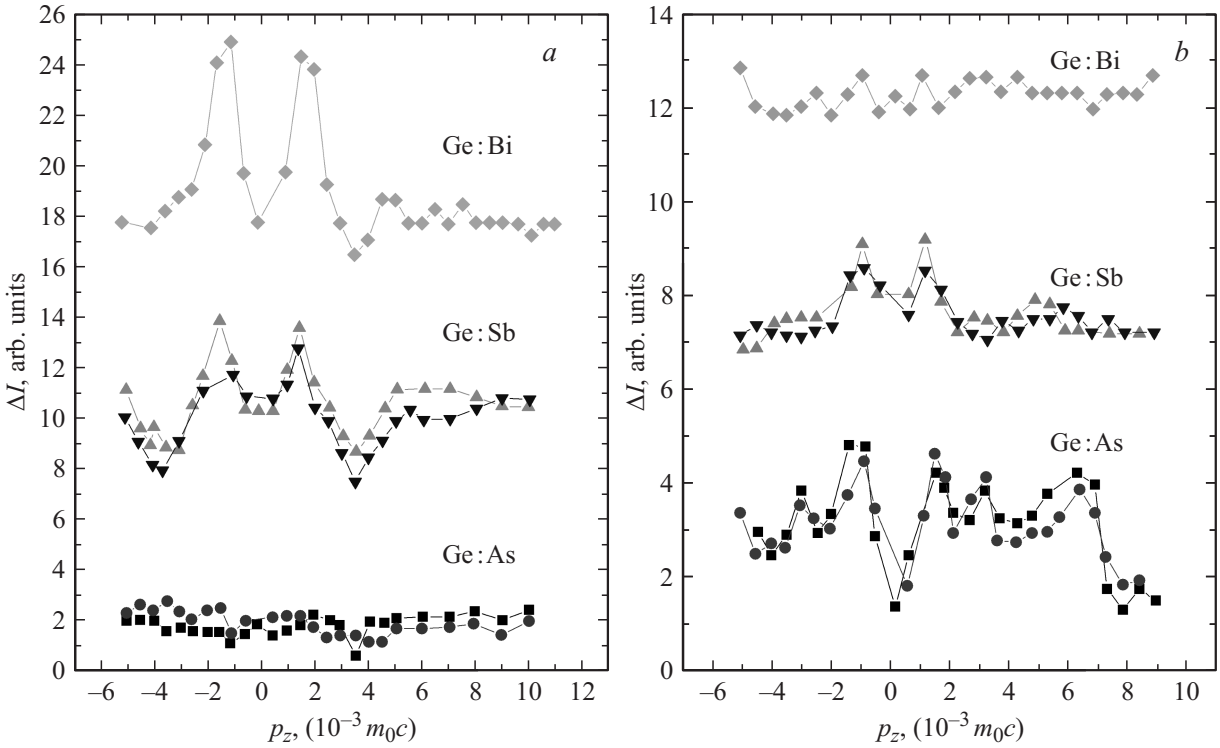

Figure 5. *a* — difference curves of 1D-ACAR for the [111] crystallographic direction of the irradiated *n*-Ge before $n \to p$ conversion: *n*-Ge : As, gamma-irradiated(squares) and neutron-irradiated (circles); *n*-Ge : Sb, gamma-irradiated (triangles up) and neutron-irradiated (triangles down); *n*-Ge : Bi, gamma-irradiated (diamonds). The difference curves of 1D-ACAR for the irradiated *n*-Ge are obtained with reference to those for the non-irradiated materials. Concentration of group-*V* impurities is in a range of $\approx 6 \cdot 10^{15}\,\mathrm{cm}^{-3}$ to $1 \cdot 10^{16}\,\mathrm{cm}^{-3}$. Irradiation dose of gamma-rays was in a range of $\Phi \approx 4 \cdot 10^{18}\,\mathrm{cm}^{-2}$ to $\Phi \approx 1 \cdot 10^{19}\,\mathrm{cm}^{-2}$. Irradiation dose of fast neutrons was $\approx 10^{13}\,\mathrm{cm}^{-2}$. Curves are displaced along the ordinate axis for clarity. *b* — difference curves of 1D-ACAR for the [110] crystallographic direction of the irradiated *n*-Ge before $n \to p$ conversion. Other details see (*a*).

n-Ge. Because of the lack of reliable information furnished by EPR the modeling of interactions between shallow donors and intrinsic point defects in *n*-Ge usually leans upon what is known about impurity-related defects in irradiated *n*-Si grown by the floating-zone technique; hereafter *n*-Si(FZ). In the latter case the trapping of vacancies at group-*V* impurity atoms is of primary importance for appearance of electrically active complexes, the so-called *E*-centers [8,9]. They were proved to be deep acceptors at $\approx E_C - 0.4\,\mathrm{eV}$. In sharp contrast, we have concluded that the dominant impurity-related defects formed in irradiated *n*-Ge are electrically neutral. We argue that the radiation-produced acceptors at $\approx E_C - 0.2\,\mathrm{eV}$ may not be taken as being such vacancy-donor pairs because of their delayed formation kinetics; see Figs. 1 to 3. Actually, such behavior is at variance with what is expected for the reaction between negatively charged vacancies, V^- or V^{2-}, and positively charged group-*V* impurity substitutional atoms D_s^+. Therefore, one must consider other ways for getting an insight into the nature of the dominant radiation defects in *n*-Ge. Among the appropriate experimental techniques being sensitive to vacancy-related defects, positron annihilation spectroscopy appears to be useful, especially measurements of the angular correlation of annihilation radiation in one dimension (1D-ACAR); a comprehensive description of the technique and data processing can be found in [10,11]. The basics of such measurements may be sketched in the following way. Positrons emitted from a positron source of ^{22}Na are incident upon Ge samples. The highly energetic positrons lost their energy in collision and ionization processes in a matter of a few 10^{-12} s. Taking into account that the positron lifetime in Ge is of order of 10^{-10} s, it means that most positrons are thermalized during their diffusion through the lattice. They predominantly annihilate with electrons in the valence band giving rise to the so-called narrow (small angle) component of 1D-ACAR as well as with inner-shell electrons giving rise to the so-called broad (larger angle) component of 1D-ACAR. Together with this, a fraction of diffusing positrons can be trapped by vacancy-related defects having an open volume in the crystal lattice. The attractive potential for positron trapping originates from the missing lattice atoms; under normal conditions the lattice atoms prevent from positron trapping because of their repulsive force. The trapped positrons annihilate with the electrons localized in the vacancy-related defects affecting the shape of the narrow component of 1D-ACAR. These changes can be observed by comparison with the reference response of initial samples. Figs 5, *a, b* show how the shapes of the 1D-ACAR curves taken in different crystallographic axes are changed for the irradiated oxygen-lean *n*-Ge before

$n \to p$ conversion. Firstly, there is ample evidence of the presence of vacancy-related defects in irradiated *n*-Ge. Secondly, one may discriminate various group-*V* impurities involved in the vacancy-related complexes by comparison to the 1D-ACAR curves taken in the principal crystallographic axes. In other words, here we are dealing with vacancy-related complexes containing group-*V* impurity atoms. It is particularly remarkable that very similar changes in the 1D-ACAR curves were also observed in *n*-Ge irradiated with fast neutrons at low doses; see Fig. 5, *a, b*. From this it follows that at early stages of fast neutron irradiation when the effect of disordered regions is still subtle the presence of similar vacancy-related defects is well pronounced. The next question is their atomic structures. One simple configuration for such a defect may be a vacancy-donor pair, like the *E*-center in irradiated *n*-Si(FZ). These prominent defects in irradiated *n*-Si(FZ) have a well-known single acceptor state at $\approx E_C - 0.4\,\text{eV}$ [2,7,8]; besides, it has been reported that they also have a deep donor state at $\approx E_V + 0.1\,\text{eV}$ [12]. By analogy, it is widely believed in literature that such pairs should also be acceptors in irradiated *n*-Ge. In sharp contrast, the dominant radiation defects in *n*-Ge appear to be electrically neutral, as was shown above.

2.4. Annealing of dominant radiation defects in irradiated *n*-Ge before $n \to p$ conversion

Studies of the thermal stability of radiation-produced defects can provide additional important information concerning the defects. As pointed out above, there are two kinds of radiation defects whose presence in *n*-Ge before $n \to p$ conversion has been reliably established by Hall effect measurements. Hence, in annealing experiments one needs to keep track of changes in their concentrations. As an example, the data obtained during isochronal anneals of *n*-Ge : P, *n*-Ge : Sb, and *n*-Ge : Bi are shown in Figs. 6–8 where the concentration $N_{0.2}^{\text{rad}}$ of the radiation-

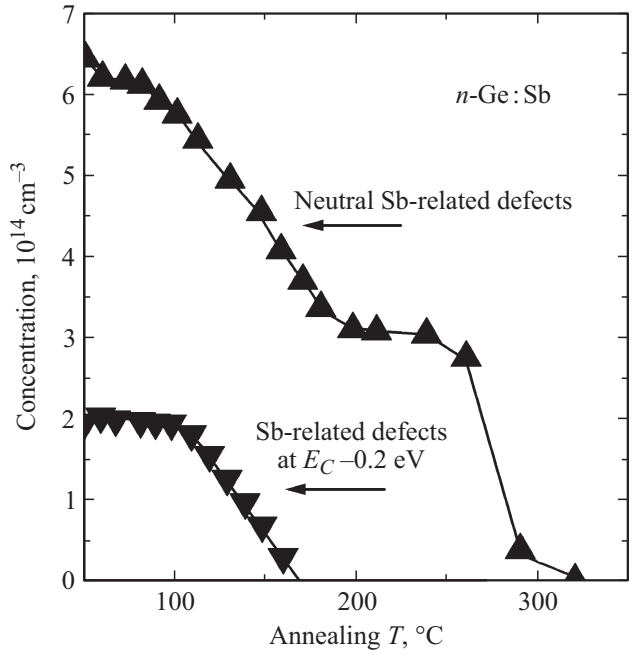

Figure 6. Isochronal annealing of electrically neutral radiation defects and acceptor defects at $\approx E_C - 0.2\,\text{eV}$ in the gamma-irradiated *n*-Ge : Sb before $n \to p$ conversion.

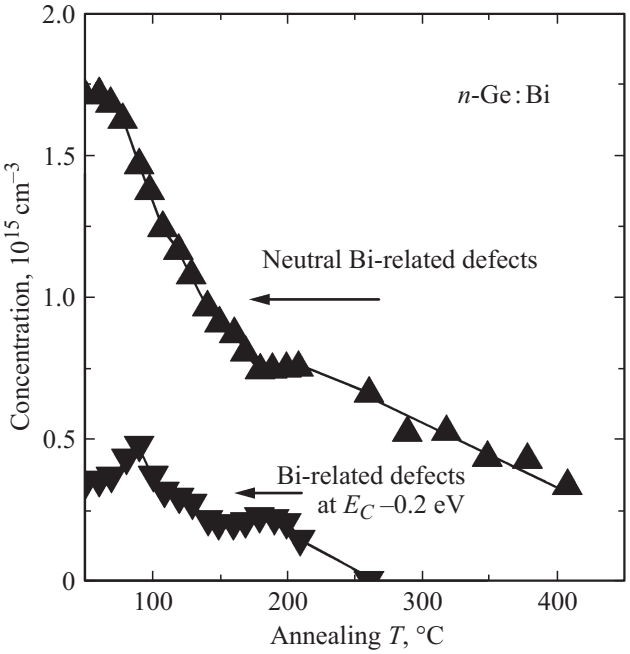

Figure 7. Isochronal annealing of electrically neutral radiation defects and acceptor defects at $\approx E_C - 0.2\,\text{eV}$ in the gamma-irradiated *n*-Ge : Bi before $n \to p$ conversion.

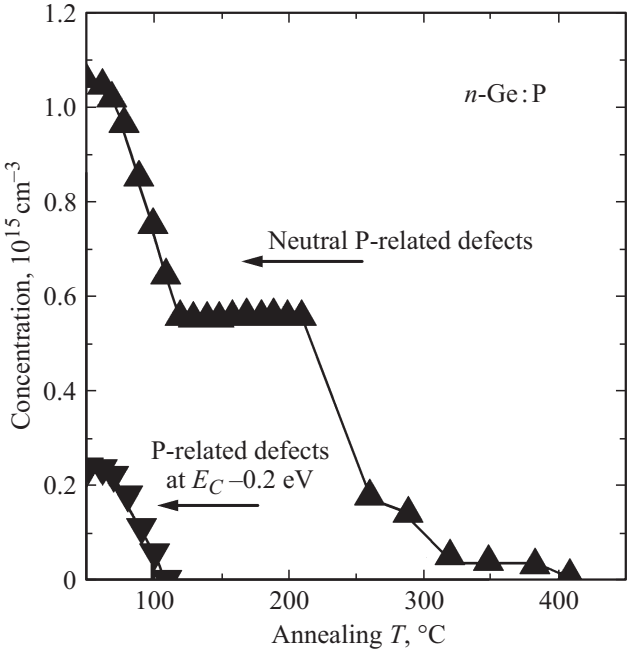

Figure 8. Isochronal annealing of electrically neutral radiation defects and acceptor radiation defects at $\approx E_C - 0.2\,\text{eV}$ in the gamma-irradiated *n*-Ge : P before $n \to p$ conversion.

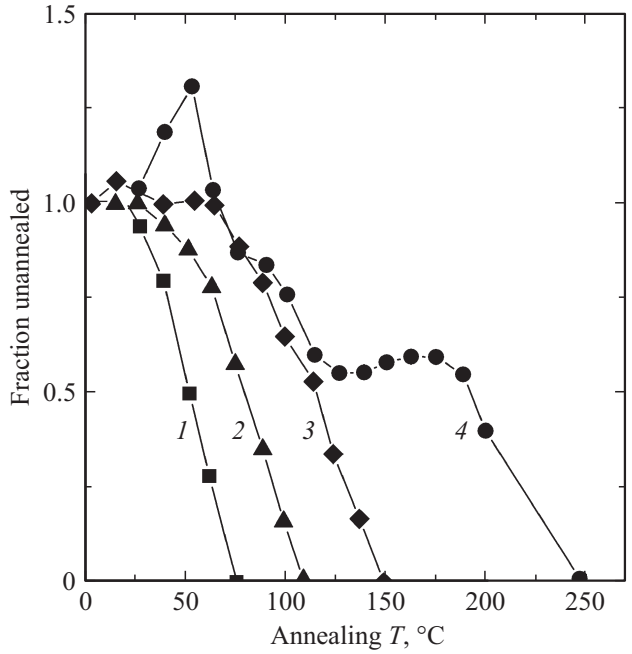

Figure 9. Isochronal annealing of radiation acceptor defects at $\approx E_C - 0.2$ eV in the gamma-irradiated *n*-Ge before $n \to p$ conversion. Samples: *n*-Ge:P (curve *1*); *n*-Ge:As (curve *2*); *n*-Ge:Sb (curve *3*); *n*-Ge:Bi (curve *4*).

produced single acceptors at $\approx E_C - 0.2$ eV as well as the concentration $N_n^{\rm rad}$ of electrically neutral complexes containing group-*V* impurity atoms (free charge carriers removed at room temperature) are plotted against the annealing temperature. Again, the annealing fraction of neutral defects is markedly greater than the annealing fraction of radiation-produced acceptors at $\approx E_C - 0.2$ eV in all of the group-*V* doped samples, thus showing the relative contribution of each defect component. It is seen that the annealing processes appear to be complicated. Let us outlined some interesting results being common for all group-*V* impurities. There are two temperature intervals of defect annealing $100^\circ\text{C} \le T \le 200^\circ\text{C}$ and $T \ge 200^\circ\text{C}$. The annealing behavior at the both intervals appears to be dependent on the chemical nature of impurities. Similarly to *n*-Si(FZ), their thermal stability increases with increasing covalent radius of impurity atoms; see Fig. 9. The annealing at the first stage produces a remarkable decrease of both $N_{0.2}^{\rm rad}$ and $N_n^{\rm rad}$. Whereas radiation acceptors at $\approx E_C - 0.2$ eV disappear completely at $T \le 200^\circ\text{C}$ (and $T \le 250^\circ\text{C}$ for *n*-Ge:Bi), the concentration of shallow donor states at the end of the first annealing stage turned out to be far from being completely restored. Making use of Hall effect measurements down to $T \approx 8$ K this was confirmed for irradiated *n*-Ge after an anneal at $T = 200^\circ\text{C}$. From this, we may conclude that among the electrically neutral radiation defects, there two kinds of impurity-related complexes having different thermal stability. Hence, the annealing story of radiation defects in *n*-Ge before $n \to p$ conversion doesn't end with the annealing of radiation acceptors at $\approx E_C - 0.2$ eV, as has sometimes suggested [13].

2.5. DLTS studies of radiation defects in irradiated *n*-Ge before $n \to p$ conversion

From the above discussion of data obtained with the help of Hall effect measurements, it follows that the dominant vacancy-related defects containing group-*V* impurity atoms appear to be electrically neutral in *n*-Ge. Unfortunately, they apparently have not been detected by DLTS as yet. Because of this, caution must be exercised in the interpretation of defect production rates based on DLTS spectra alone; see for instance [13]. In actual fact, the Hall effect data has allowed one to reliably assess the production rates of the dominant radiation defects in oxygen-lean moderately doped *n*-Ge under ^{60}Co gamma-rays irradiation: the production rate of electrically neutral complexes containing group-*V* impurity atoms was found to be greater by an order-of-magnitude than that of acceptor defects at $\approx E_C - 0.2$ eV, $(1-2) \cdot 10^{-3}$ *vs* $(1-2) \cdot 10^{-4}$ cm^{-1}, correspondingly [3,4].

Much detailed information on radiation defects in irradiated in *n*-Ge has been gained from extensive DLTS measurements [13–21]. Figs 10 and 11 present an excellent example of a much pronounced shift of the DLTS peaks associated with electron and hole traps containing various group-*V* impurity atoms in irradiated *n*-Ge [16]. Comprehensive DLTS and LDLTS studies taken on irradiated oxygen-lean *n*-Ge before $n \to p$ conversion have made it possible to determine some important electronic parameters of the electron traps (see Fig. 10), among them the activation energies of electron emission and electron capture etc. A combined analysis of data obtained has allowed one to derive the enthalpy ΔH and entropy ΔS as well as the

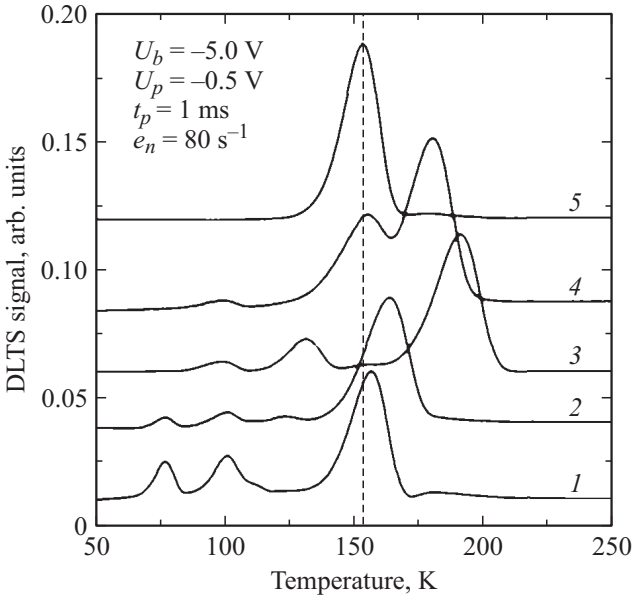

Figure 10. DLTS spectra for gamma-irradiated oxygen-lean Ge crystals doped with P (*1*), As (*2*), Sb (*3*), and Bi (*4*). Spectrum 5 was recorded on a gamma-irradiated oxygen-rich Ge sample. The spectra have been vertically displaced for clarity. Measurement settings were $e_n = 80\,\text{s}^{-1}$, bias $U_p - 0.5$ V, and pulse duration 1 ms. Data are taken from [16].

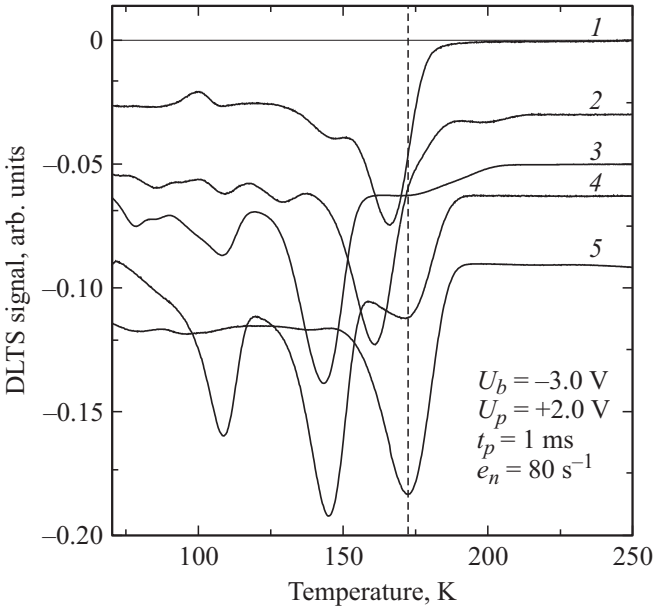

Figure 11. Injection DLTS spectra for gamma-irradiated oxygen-lean Ge crystals doped with P (*1*), As (*2*), Sb (*3*), and Bi (*4*). Spectrum 5 was recorded on a gamma-irradiated oxygen-rich Ge sample. The spectra have been vertically displaced for clarity. Measurement settings were $e_n = 80\,\mathrm{s}^{-1}$, bias $U_p + 2.0$ V, and pulse duration 1 ms. Data are taken from [16].

Gibbs free energy ΔG of the defect ionization in *n*-Ge doped with the various group-*V* impurities [16–18]. The ΔH values indicate convincingly that they are impurity-dependent, as also the ΔS values. Surprisingly, the entropy factors ΔS being of several k turned out to be significantly higher than those found for defects in Si which are usually $\Delta S \leq k$ where k is Boltzmann's constant. In view of the high entropy values, the energy level of these electron traps is expected to be temperature-dependent, so the ΔG values should be close to 0.2 eV over a temperature interval of $T \approx 200$ to 300 K. This correlates well with the Hall effect measurements; see Fig. 1. In addition, the annealing behavior of the acceptor defects at $\approx E_C - 0.2$ eV studied by DLTS was found to be impurity-dependent [16], also in good agreement with Hall effect data; see Fig. 10. A pronounced negative annealing of acceptor defects at $\approx E_C - 0.2$ eV in the *n*-Ge : Bi observed in the studies by Hall effect measurements [4] and DLTS [16] can be attributed to annealing of oxygen-vacancy pairs (the so-called *A*-centers) at temperatures around 100°C accompanied with an additional formation of vacancy-related complexes containing Bi atoms; see also below.

Along with the above characteristics of acceptor defects at $\approx E_C - 0.2$ eV, it was found that the multiphonon-assisted capture of electrons at these deep centers is dependent on the chemical nature of group-*V* impurity in the complex, with the energy barrier for capture $\Delta E_{n\sigma}$ and the capture cross section σ_{n0} at $1/T = 0$ being in the range of $\Delta E_{n\sigma} = 0.065$ to 0.085 eV and $\sigma_{n0} = 1.6 \cdot 10^{-16}$ to $9.2 \cdot 10^{-17}$ cm^2 [16].

An investigation of minority carrier traps in irradiated *n*-Ge revealed the presence of prominent radiation-produced hole traps exhibiting field-enhanced hole emission and this, in turn, allowed one to attribute them to acceptor centers [14–16]. The activation energy for hole emission of about 0.3 eV turned out to be dependent also on the chemical nature of group-*V* impurities; see Fig. 11 [16]. Taking into account that the both dominant electron and hole traps are annealed in a similar way, it has been suggested that they are associated with a single defect which is a double acceptor. What is more, a thorough analysis of spectra recorded on Sb in-diffused n^+-p-mesa diodes with the aid of high resolution LDLTS allowed one to find an additional line reportedly related to neutral radiation-produced defects with an ionization enthalpy of $\Delta H_p = (0.095 \pm 0.006)$ eV whose donor states are placed close to the valence band [21,22]. Again, a close similarity in the annealing behavior of the defects with acceptor and donor states in the lower half of the band gap led to the conclusion that this vacancy-related complex is an amphoteric defect with two acceptor states and a single-donor state; see Fig. 12.

As compared to the *E*-center Si with a single-acceptor [8,9] and single-donor states [22], it seems amazing that the same structural complex in Ge is thought to introduce three energy states in the band gap that is narrower by 40 percent. However, the suggested model of the defects as being vacancy-impurity pairs provides some serious objections. First, their *delayed* formation kinetics is not consistent with an effective trapping process of negatively charged vacancies at positively charged impurity atoms. Second, the energy barrier for electron trapping at acceptor defects at $\approx E_C - 0.2$ eV may be formed by the atomic structure itself and not necessarily due to the presence of a negatively charged states. Third, the annealing processes of radiation-produced defects in *n*-Ge before $n \rightarrow p$ conversion are rather complicated and some of them are running concurrently. Because of this a reliable analysis of production and annealing processes of defects under

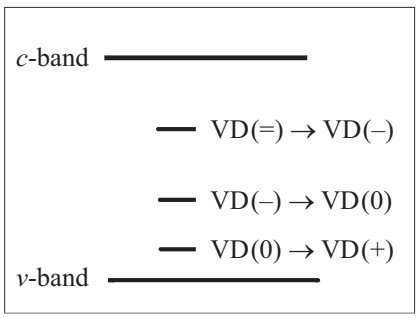

Figure 12. Principal scheme of charge states taken as belonging to the vacancy — group-*V* impurity atom complex (the *E*-center) in Ge. The charge state of the pair VD depends on the Fermi level position. Exact positions of acceptor states of the complex in the band gap are dependent on the chemical nature of impurity atoms; see text.

consideration should be made on the basis of changes in their absolute concentrations in order to assess contributions of individual groups of radiation defects. Unfortunately, such information concerning DLTS data on irradiated Ge can be found seldom. Another problem associated with defect modeling based on DLTS alone is that the dominant neutral radiation-produced defects in *n*-Ge responsible for the major degradation of its electrical parameters should not be observable. That is why a problem of production rates of impurity-related defects in irradiated *n*-Ge before $n \to p$ conversion, closely associated with estimates of primary defect production, cannot be treated in a proper way solely relying on DLTS data. For similar reasons, in irradiated *n*-Ge before $n \to p$ conversion the defect annealing at $T > 200^\circ$C has mostly been beyond the consideration in DLTS papers. Because of this, observation of the disappearance of the dominant electron and hole traps upon isochronal annealing of electron-irradiated *n*-Ge:Sb at $T = 75^\circ$C to 175°C, accompanied with the formation of other hole traps in the lower part of the band gap, has awakened fresh interest, since the latter traps are annealed out at $T = 300^\circ$C [17]; *cf* Fig. 6. It is also worth noting that DLTS data obtained on proton-irradiation of *n*-Ge:Sb [14] suggest several kinds of Sb-related radiation defects.

2.6. Kinetics of defect formation in irradiated *n*-Ge after $n \to p$ conversion

As the gamma-irradiation dose of moderately doped oxygen-lean *n*-Ge continues to increase, the irradiated material gradually turns intrinsic and then, after prolonged irradiation, it changes its conductivity type from *n* to *p*. The surprising thing is that the hole concentration at room temperature after prolonged irradiation approaches the initial concentration of shallow donors in the original low-doped material; see also [3]. Extensive Hall effect measurements have made it possible to establish the formation of radiation defects with energy states near the valence band. It is of keen interest that the positions of these levels were found to be dependent on the chemical nature of the group-*V* impurities being present in initial materials, namely, $E_V + 0.10$ eV for *n*-Ge:P and *n*-Ge:As as well as $E_V + 0.12$ eV for *n*-Ge:Sb, and $E_V + 0.16$ eV for *n*-Ge:Bi where E_V is the valence band. As an illustration, one typical curve of the hole concentration *vs* reciprocal temperature, $p(1/T)$, as well as the formation kinetics of defects at $E_V + 0.12$ eV in the irradiated *n*-Ge:Sb after $n \to p$ conversion is displayed in Figs. 13 and 14. In sharp contrast, the production rate of these defects turns out to be very low, about $7 \cdot 10^{-5}$ cm^{-1} which is by a factor of 20 less than that observed in *n*-Ge before $n \to p$ conversion; see above. Certainly, this reflects a very pronounced difference in the direct annihilation and separation processes of Frenkel pairs as primary defects in *n*- and *p*-type materials, on the one hand, and in indirect annihilation processes of free vacancies and self-interstitials if there are energy barriers for their trapping at impurity-related defects, on the other. Concerning the electrical

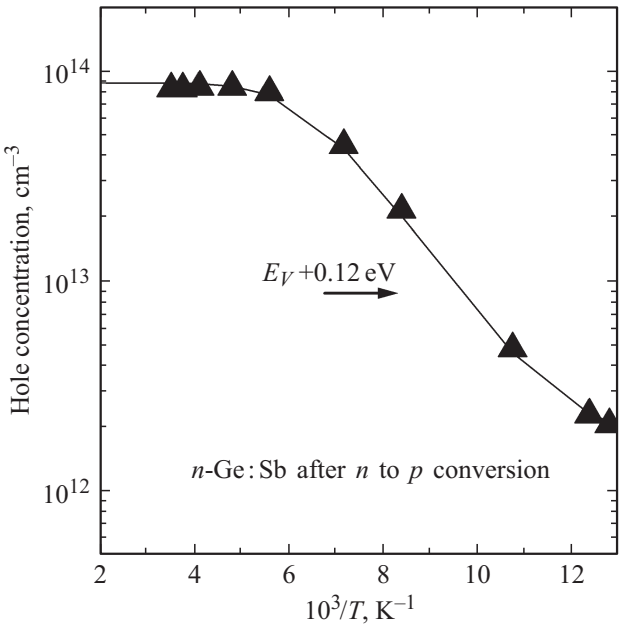

Figure 13. Hole concentration *vs* reciprocal temperature for the irradiated *n*-Ge:Sb after $n \to p$ conversion. Points, experimental; curves, calculated. Dose Φ, $1.2 \cdot 10^{18}$ cm^{-2}. Ionization energy of radiation-produced defects is indicated.

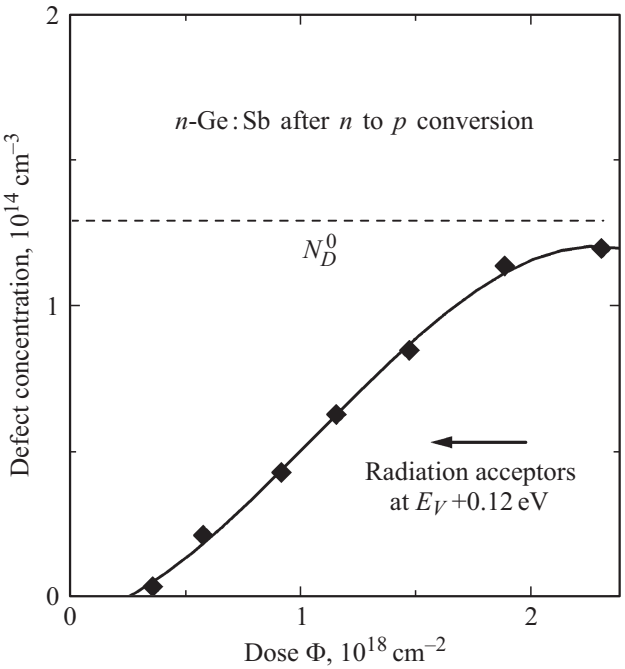

Figure 14. Formation kinetics of radiation acceptor defects at $E_V + 0.12$ eV in the irradiated *n*-Ge:Sb after $n \to p$ conversion. N_D^0 shows the initial concentration of group-*V* impurity.

activity of these dominant defects we have arrived at the preliminary conclusion that they should be of acceptor type, since, together with them, there are shallower acceptor states whose presence at the saturation plateau of curves $p(1/T)$ is evident around $T \approx 78$ K. This conclusion is

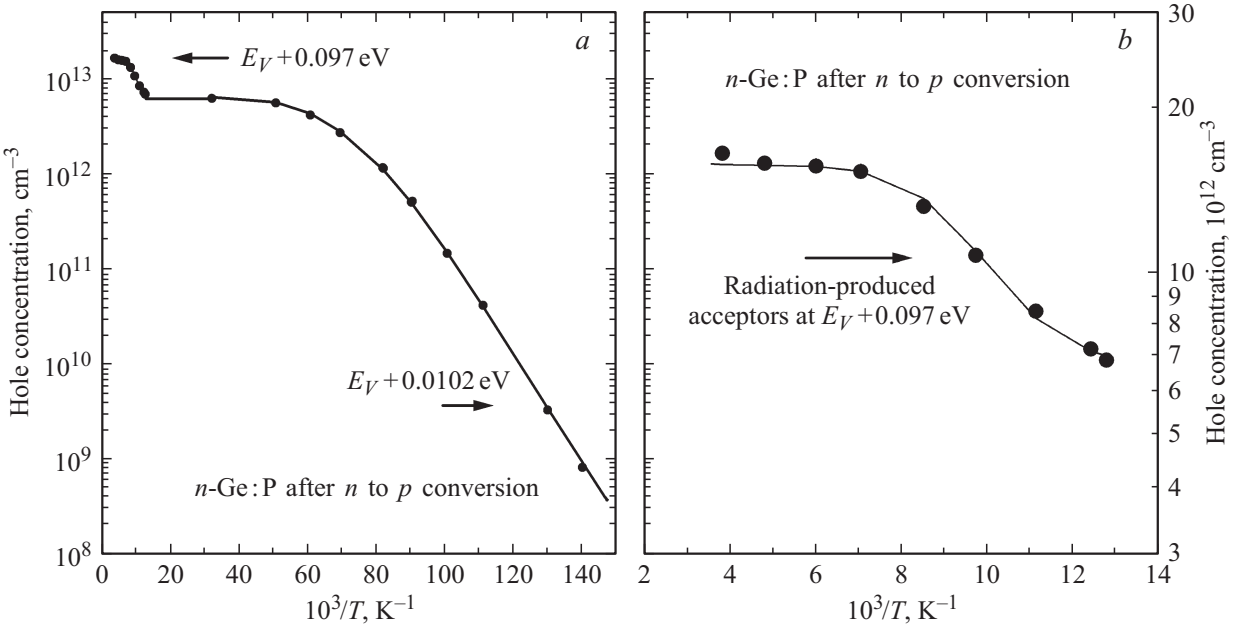

Figure 15. *a* — hole concentration *vs* reciprocal temperature for the gamma-irradiated *n*-Ge:P after $n \to p$ conversion at an ultimate state. Points, experimental; curves, calculated. Dose Φ, $4.6 \cdot 10^{17}$ cm^{-2}. Parameters after the irradiation: $E_A = 10.2$ meV; $N_A^{\mathrm{III}} = 8.60 \cdot 10^{12}$ cm^{-3}; $\beta_A = 1/4$; $N_D = 2.10 \cdot 10^{12}$ cm^{-3}. Concentrations of radiation acceptor defects in the irradiated sample: $N_A^{\mathrm{rad}} = 9 \cdot 10^{12}$ cm^{-3} ($E_V + 97$ meV). *b* — hole concentration *vs* reciprocal temperature for the gamma-irradiated *n*-Ge:P after $n \to p$ conversion at an ultimate state, displayed on the expanded scale. Points, experimental; curves, calculated. Dose Φ, $4.6 \cdot 10^{17}$ cm^{-2}. The parameters of the calculated line are the same as in (*a*). Other parameters see in (*a*).

sustained by Hall effect measurements taken at cryogenic temperatures down to $T \approx 7$ K.

2.7. Low-temperature Hall effect measurements on irradiated *n*-Ge after $n \to p$ conversion

Some interesting information has been furnished by electrical measurements at cryogenic temperatures. As an example, in Fig. 15, *a, b* we show $p(1/T)$ curve for one of the irradiated *n*-Ge samples after $n \to p$ conversion when this irradiated sample had reached an ultimate state. The presence of two energy states at $E_V + 0.097$ eV and $E_V + 0.0102$ eV is evident. The latter one can reliably be identified as the shallow acceptors of Al being partially compensated by deep donors. This $p(1/T)$ curve over a temperature range of $7\,\mathrm{K} \le T \le 50\,\mathrm{K}$ can be analyzed making use of an equation of charge balance, in a similar way as we did earlier in the case of *n*-type Ge,

$$\frac{p(p+N_D)}{N_A - N_D - p} = \beta_A N_V T^{3/2} \exp\left(-\frac{E_A}{kT}\right)$$

where N_V is the effective density-of-states of the valence band, E_A and β_A are the ionization and degeneracy factor of the ground states of shallow acceptors, respectively; the contribution of the third split-off valence band can be ignored because of the large splitting from the valence bands of light and heavy holes; other symbols have their usual meanings. All remarks related to concentrations of electrically active centers in *n*-Ge still stand for *p*-Ge as well by relevant substitution for $n \to p$, N_D^V (shallow group-*V* donors) $\to N_A^{\mathrm{III}}$ (shallow group-III acceptors), and N_A (compensating deep acceptors) $\to N_D$(compensating deep donors). The analysis makes it apparent that the total concentration of shallow acceptors is nearly equal to the concentration of trace compensating acceptors in the initial *n*-Ge. (DLTS measurements on the initial material showed that the concentration of deep centers didn't exceed 10^{11} cm^{-3}.) The presence of partially compensated shallow acceptors in low concentration tells us immediately that dominant energy states at $E_V + 0.097$ eV are also acceptors. Similar conclusions were also verified for the other group-*V* impurities in irradiated *n*-Ge after $n \to p$ conversion, too. Therefore, after this conversion the reactions between group-*V* impurity atoms and intrinsic point defects result in the appearance of radiation-produced acceptor defects at $\approx E_V + 0.1$ eV in concentration close to the initial shallow donor concentration in *n*-Ge. In actual fact, this is in sharp contrast to what is known for defect reactions in irradiated *n*-Si(FZ). It will be recalled once again that looking for close similarities in properties and behavior of radiation-produced defects in Si and Ge may be in some instances misleading.

2.8. On the nature of dominant radiation defects in irradiated *n*-Ge after $n \to p$ conversion

The defect formation in *n*-Ge after $n \to p$ conversion brings up another point concerning the nature of the dominant radiation-produced defects. Here, the situation

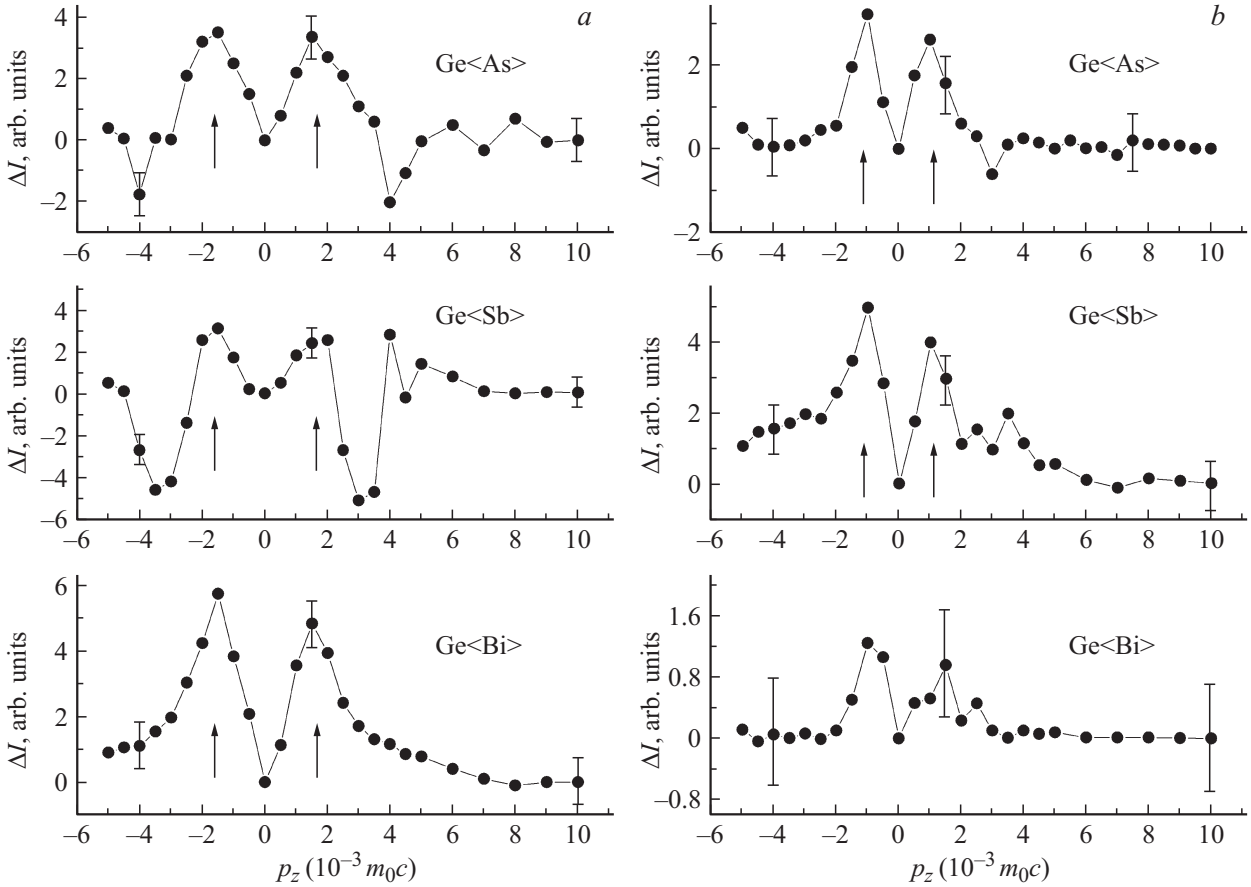

Figure 16. *a*). Difference curves of 1D-ACAR for the [111] crystallographic direction of the irradiated *n*-Ge after $n \to p$ conversion. The difference curves of 1D-ACAR for the irradiated *n*-Ge are obtained with reference to those for the non-irradiated materials. Irradiation dose of gamma-rays was in a range of $7 \cdot 10^{18}$ cm^{-2} to $2 \cdot 10^{19}$ cm^{-2}. *b*). Difference curves of 1D-ACAR for the [110] crystallographic direction of the irradiated *n*-Ge after $n \to p$ conversion.

appears to be simpler than that for *n*-Ge before $n \to p$ conversion. Again, it is instructive to apply positron annihilation spectroscopy to the materials converted to *p*-type by prolonged irradiation. The results are shown in Fig. 16, *a, b* where the difference curves of 1D-ADAP are plotted for the *n*-Ge : P, *n*-Ge : Sb, and *n*-Ge : Bi after $n \to p$ conversion. First of all, it is seen that the irradiation affects strongly the shape of the narrow components. This, in turn, provides convincing evidence that the complexes studied are vacancy-related. Along with this, the shapes of the 10-ADAP curves are sensitive to the chemical nature of group-*V* impurity in a different way than those recorded for *n*-Ge before $n \to p$ conversion; *cf* Figs. 5 and 16. Therefore, taking into consideration the information discussed in Sections 2.7 and 2.8 it may be inferred that the dominant radiation-produced defects in *n*-Ge after $n \to p$ conversion are also vacancy-related complexes containing one group-*V* impurity atom per each complex.

2.9. Annealing of dominant radiation defects in irradiated *n*-Ge after $n \to p$ conversion

In conformity with our observation of the dominant formation of radiation defects of one kind in irradiated *n*-Ge

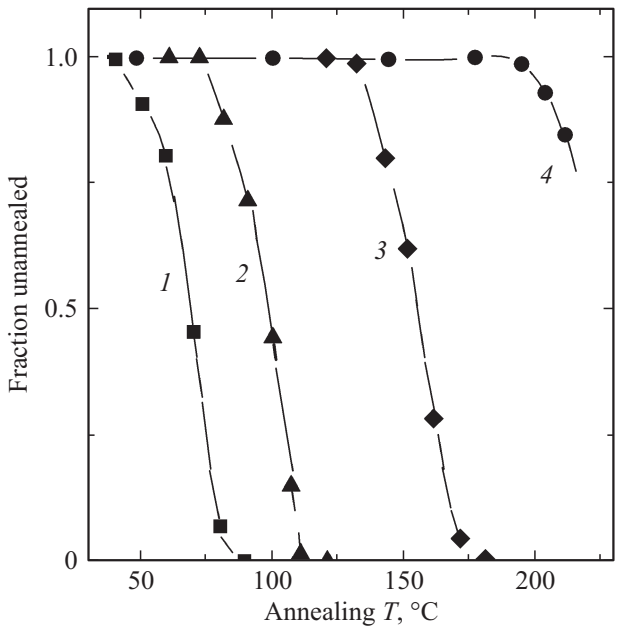

Figure 17. Isochronal annealing of radiation acceptor defects at $\approx E_V + (0.10-0.16)$ eV in gamma-irradiated *n*-Ge after $n \to p$ conversion. Samples: *n*-Ge : P (curve *1*); *n*-Ge : As (curve *2*); *n*-Ge : Sb (curve *3*); *n*-Ge : Bi (curve *4*).

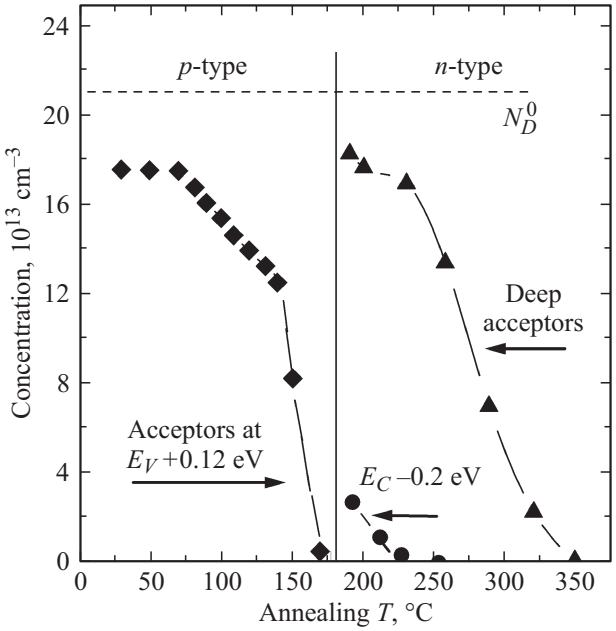

Figure 18. Isochronal annealing of the gamma-irradiated *n*-Ge : Sb after $n \to p$ conversion. The sample was converted to *p*-type by the irradiation and then it returned to *n*-type in the course of the isochronal annealing. N_D^0 shows the initial concentration of group-*V* impurity.

after $n \to p$ conversion, their annealing was found to occur at one stage. As is seen in Fig. 17, the temperature interval of defect annealing processes turned out to be dependent on the chemical nature of group-*V* impurity. Again, their thermal stability is increased with increasing covalent radius of impurity atoms, as is earlier observed in the case of radiation-produced defects in irradiated *n*-Ge before $n \to p$ conversion; see Fig. 9. As our Hall effect data obtained at cryogenic temperatures suggest, the decay process of the dominant acceptor defects at $\approx E_V + 0.1$ eV during the annealing is accompanied by restoration of shallow donor states, so just after $p \to n$ conversion the latter ones are free but strongly compensated by deep acceptors; see Fig. 18. Based on this observation we believe that the decay process consists in decomposition of the complex leaving a free impurity atom and a deep acceptor being another constituent as the whole entity or a part of it. Some peculiarities of these annealing processes in irradiated *n*-Ge : P, As, and Bi after $p \to n$ conversion invite further detailed investigation.

2.10. Role of oxygen in defect formation in irradiated *n*-Ge

Though the concentration of dissolved oxygen in Ge crystals grown by the Czochralski technique is usually by an order-of-magnitude less than that in Si also grown by the same technique, the picture of defect reactions in irradiated *n*-Ge is strongly affected if the concentration of oxygen in the material is in a concentration range of $\approx 5 \cdot 10^{16}$ cm^{-3} to $\approx 3 \cdot 10^{17}$ cm^{-3}. First of all, considerable interest is attracted to trapping of mobile vacancies at oxygen atoms resulting in formation of oxygen-vacancy pairs, the so-called *A*-centers as in the nomenclature of defects in irradiated Si [2,23]. These defects have been extensively studied by Hall effect measurements and DLTS spectroscopy; see for instance [24–26] and the literature contained therein. There, Hall effect measurements on irradiated oxygen-rich *n*- and *p*-Ge have revealed two dominant oxygen-related defects whose energy states are at $\approx E_C - 0.24$ eV and $\approx E_V + 0.27$ eV, correspondingly [26]. This information correlates well with the electronic properties of the dominant oxygen-related electron and hole traps observed in oxygen-rich irradiated *n*-Ge by DLTS and LDLTS [26]. It is argued on the basis of the collected data that the *A*-center in Ge has the two acceptor states indicated above. This conclusion was amplified by results obtained by high-resolution vibrational mode infrared spectroscopy [24,25]. Three absorption bands at 621, 669, and 716 cm^{-1} are ascribed to the asymmetric stretching local vibrational modes of *A*-centers which, in turn, are associated with three charge states of the *A*-center (neutral, single negative, and double negative ones, respectively). A very much pronounced difference in the behavior of oxygen-rich and oxygen-lean *n*-Ge under irradiation can be illustrated in Fig. 19 where the concentration of acceptor defects in the *n*-Ge after $n \to p$ conversion is plotted against irradiation dose. As mentioned earlier, the concentration of oxygen in some Bi-doped samples ($\sim 8 \cdot 10^{15}$ cm^{-3}) was higher than the other group-*V* doped samples and clear evidence of its emerging relative role in the defect

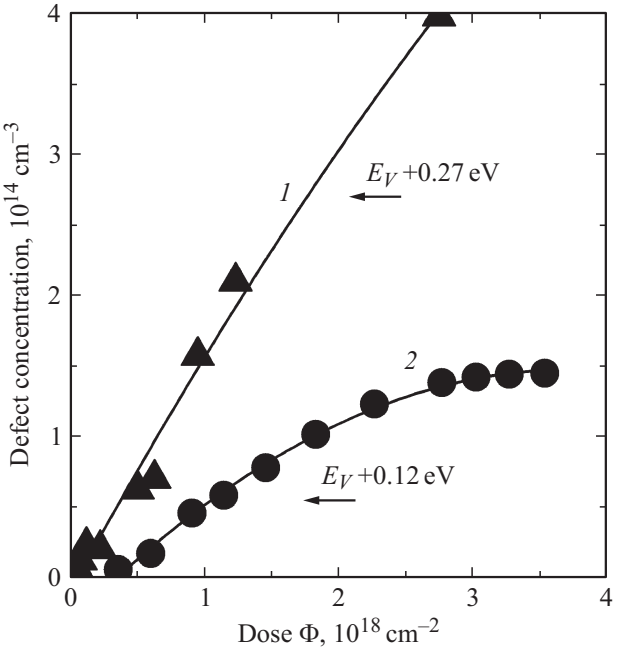

Figure 19. Concentration of radiation-produced acceptor defects *vs* irradiation dose in oxygen-rich and oxygen-lean *n*-Ge after $n \to p$ conversion. Curve *1*, undoped *n*-Ge ($n \approx 1 \cdot 10^{13}$ cm^{-3}); curve *2*, *n*-Ge : Sb, $N_D^0 = 1.4 \cdot 10^{14}$ cm^{-3}. Oxygen concentration, cm^{-3}: $3 \cdot 10^{16}$ (curve *1*); $2 \cdot 10^{15}$ cm^{-3} (curve *2*).

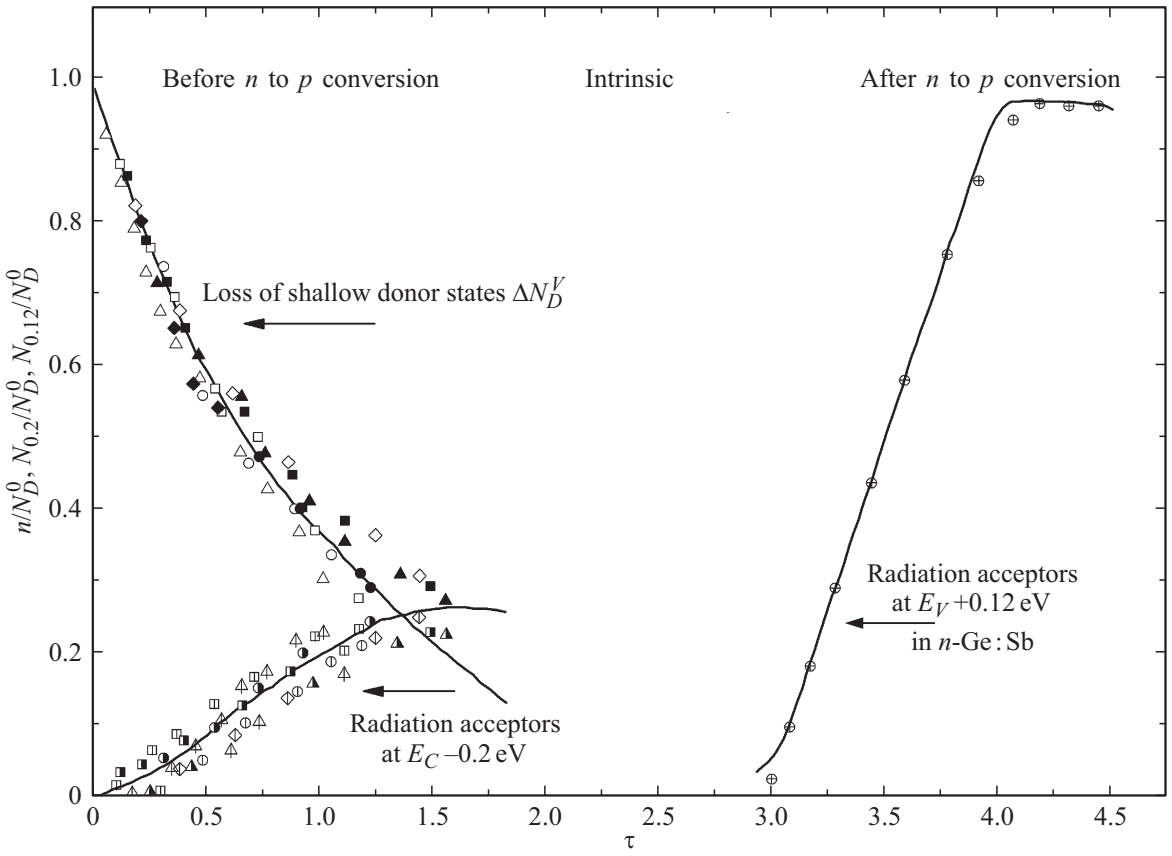

Figure 20. Comparison of the experimental and calculated dose dependences of the relative concentrations of group-V impurity atoms and radiation-produced acceptor defects. Points, experimental; curves, calculated. Group-V impurities: P, As, Sb, and Bi in a concentration range of $1.1 \cdot 10^{14}$ to $2.8 \cdot 10^{15}$ cm^{-3}. $\Delta n\,(T = 300\,\mathrm{K}) \approx \Delta N_D^V$ (see text). All relative concentrations are given in respect to the initial concentrations of shallow donors, N_D^0. Dimensionless time of gamma-irradiation, $\tau = \lambda t / N_D^0$ where $\lambda = \sigma J N_{at}$ is the generation rate of free vacancies (σ is the cross-section of generation of separated Frenkel pairs; J is the intensity of gamma-irradiation; N_{at} is the concentration of regular atoms in Ge); t is the duration of gamma-irradiation. Remember that the generation rate of free vacancies after $n \to p$ conversion is by a factor of 20 less than that before $n \to p$ conversion (see text). In the model of successive trapping of vacancies it is assumed that the vacancy-donor pair is neutral in n-Ge. The divacancy-donor complex is thought to be associated with acceptors at $\approx E_C - 0.2$ eV and the high entropy factors may be due to a larger open volume of the defects (see text). The tetravacancy-donor complex is ascribed to acceptors at $\approx E_V + (0.1{-}0.16)$ eV. Trivacancy-donor complexes may be deep centers being unobservable by Hall effect measurements in irradiated material having intrinsic conductivity. This model may be used for phenomenological purposes. For details see [5].

processes has been observed. This is apparent in the annealing of the $\approx E_C - 0.2$ eV acceptor level in Figs. 7 and 9. There a significant increase in its concentration is observed at $T \gtrsim 100^\circ$C, where the A-center is known to disappear [24] and release its vacancy for re-trapping; see also [16]. Also in some irradiated samples of n-Ge : Bi with such oxygen concentrations the formation of oxygen-related defects at $\approx E_V + 0.27$ eV after $n \to p$ conversion is observed in parallel to the formation of the vacancy-related complexes at $E_V + 0.16$ eV. Therefore, identification and modeling of radiation-produced defects in n-Ge should be made with caution taking into account the possible active role of oxygen in the defect reactions. In the past, the presence of oxygen in noticeable concentration has often led to a conflicting situation with interpretation of Hall effect data on irradiated moderately doped n-Ge, since the formation of A- and E-centers went on concurrently but the appearance of A-centers with acceptor states at $\approx E_C - 0.24$ eV made it impossible to separate them from donor-related complexes at $\approx E_C - 0.2$ eV. At present the DLTS techniques are successful in solving such problems; see for instance Fig. 10 and [16].

3. Modeling of radiation defects in n-Ge

Previous efforts to gain a more penetrating insight into the nature of radiation-produced defects in Ge may be divided into two approaches. On the one hand, attempts have been made to simulate the experimentally observed kinetics of defect formation in irradiated n-Ge on the basis of a *preset* scheme of defect reactions. On the other hand, theoretical calculations of the expected atomic configurations of intrinsic and impurity-related defects as

well as their energy spectra and optical characteristics have been performed as an independent guide as to possible interpretatiens of the results. In both approaches, the known defect reactions in Si have formed a tempting starting point for consideration, particularly including the similarities and differences of the electrical and optical properties of known defects in Si and Ge.

In the first approach, the modeling scheme has mostly considered vacancy-related defect reactions, although free vacancies and self-interstitials in *n*-Ge are assumed to be mobile at room temperature. The role of self-interstitials in the formation of electrically active defects in *n*-Ge, say, complexes with oxygen atoms [27,28], is often thought to be of minor importance due to the formation of electrically neutral complexes like di-interstitials, etc. On the other hand, mobile vacancies are expected to be trapped at impurity atoms, for the most part at group-*V* impurity atoms in oxygen-lean *n*-Ge, thus forming vacancy-impurity complexes. This identification is in line with the results of positron annihilation spectroscopy. Coulombic attraction between negatively charged vacancies and positively charged shallow donors should strongly enhance this reaction. Therefore, just at the beginning of irradiation these defects should be dominant in oxygen-lean *n*-Ge, as in irradiated *n*-Si(FZ) [8,9]. However, the *delayed* initial formation kinetics of acceptor defects at $\approx E_C - 0.2\,\text{eV}$ appears to be inappropriate for such modeling; see Figs. 1–3. Instead, the electrically neutral defects which initiate the major changes of charge carrier concentration under irradiation merit more attention than has been accorded them previously. Taking into consideration all of the possible formation processes of radiation-produced defects in *n*-Ge before and after $n \to p$ conversion one conceives the basic idea of vacancy agglomerating at group-*V* impurity atoms in *n*-Ge. As an example, the kinetics of successive trapping of vacancies at group-*V* impurity atoms in irradiated *n*-Ge could be reasonably fitted the observed changes in concentrations of radiation-produced defects; see Fig. 20; for details see [5]. If so, the behavior of radiation defects in *n*-Si and *n*-Ge differs greatly.

Let us now consider the results of spin-density functional modeling studies of vacancy-donor pairs in Ge making use of supercell (periodic) and cluster (non-periodic) calculations [29-32]. The results point out that the group-*V* atom in the complex of [VP], [VAs], [VSb], and [VBi], where V denotes the vacancy, assumes the expected *E*-center configuration of a nearby substitutional site for all the impurities, (including Sb and Bi, in contrast to earlier calculations [33] where the heavy impurity atom was located between two semi-vacancies in the split-vacancy configuration). The predicted energy level structure of the *E*-centers involved four charge states as shown in Fig 12, whose positions depended upon the chemical nature of group-*V* impurity.To summarize briefly, the acceptor levels of the complexes were calculated to be at $\approx E_C - 0.3\,\text{eV}$ and $E_V + 0.3\,\text{eV}$, whereas their donor levels were placed close to the valence band, at $\approx E_V + 0.1\,\text{eV}$. Concerning the possible model of successive trapping of vacancies at group-*V* impurity atoms in Ge it would be interesting to calculate the energy level structure of such multivacancy complexes and their atomic configurations, especially for the heavier impurity atoms like Sb and Bi. Of possible interest is that [34] has predicted that the complex containing two vacancies and one As impurity atom in Ge should be energetically preferable in the atomic configuration of [AsVV] rather than in [VAsV].

Although all the levels indicated above have been observed by DLTS it should be noted that the model of *E*-centers under consideration seems not to be in line with the electrical data collected so far. The first point is concerned with the double acceptor states of *E*-centers. In actual fact, there is a close correlation between acceptor defects at $\approx E_C - 0.2\,\text{eV}$ seen by Hall measurements and the dominant electron traps detected by DLTS in reference to their electrical levels as well as their annealing behavior. However, according to Hall effect data these defects seem to be single acceptors. Additionally, their formation kinetics strongly differs from that one could expect for *E*-centers; cf the formation kinetics of *E*-centers in irradiated oxygen-lean *n*-Si where these dominant defects are observed to form just from the beginning of irradiation [8,9,35]. The behavior of hole traps at $\approx E_V + 0.3\,\text{eV}$ seen by DLTS in electron-irradiated *n*-Ge : Sb is unexpected for *E*-centers, since they are more dominant in materials with decreasing concentration of Sb [20]. The behavior of the hole traps at $\approx E_V + 0.09\,\text{eV}$ seems to be open to question, too [20]. Along with this, the defects being observable in irradiated *n*-Ge after $n \to p$ conversion were reliably established to be acceptors, so they can't be assigned to the donor states of vacancy-group-*V* impurity atom pairs. In other words, the identification of *E*-centers in Ge invites further experimental investigations as well theoretical calculations. An objective to be pursued by future research must be to understand the nature of the dominant impurity-related defects remaining unobserved in the DLTS and Hall effect measurements for a long time. Since the data obtained by positron annihilation spectroscopy point to the fact that they are vacancy- and impurity-related radiation defects, the important question is why these defects may be electrically neutral in irradiated *n*-Ge before $n \to p$ conversion, in sharp contrast to irradiated *n*-Si(FZ). The complexes may not be easily accessible to observation if they are deep donors having an energy barrier that prevents the trapping of charge carriers. As an extreme case, ion pairing of a negatively charged vacancy and positively charged shallow donor may not give rise to a bound electronic state in the band gap if the energy level of vacancy as a single acceptor is placed not far from the valence band.

4. Conclusions

In this paper the present situation concerning the experimental studies of radiation-produced defects, as well as the theoretical calculations of point defects, primarily vacancy-donor pairs in *n*-Ge, has been outlined. Because of the poor identification of atomic structures of defects in Ge, defect modeling for an explanation of the experimental

results has had to be based upon the suggested similarities of dominant defect complexes in Si and Ge. However, a detailed look at the experimental data collected so far shows that such defect modeling may be misleading. Surprisingly, the dominant impurity-related defects responsible for the substantial decreases in charge carrier concentration in irradiated n-Ge before $n \to p$ conversion were found to be electrically neutral and not seen by electrical measurements. In contrast, radiation-produced acceptors at $\approx E_C - 0.2\,\mathrm{eV}$ readily seen by Hall effect and DLTS measurements on irradiated n-Ge are formed in stunted growth. Because of this, their identification as being simple vacancy-donor pairs (E-centers) is questionable. There is no doubt that all of the directly observed electron and hole traps found in irradiated n-Ge are real. The problem is a matter of their absolute concentrations and relationship to the dominant radiation-produced defects. Their annealing behavior reveals the complexity of the defect reactions in n-Ge before and after $n \to p$ conversion. Positron annihilation experiments provide conclusive evidence that the dominant radiation-produced defects making their appearance before and after $n \to p$ conversion are vacancy-related complexes containing group-V impurity atoms. Combining this conclusion with the results of electrical measurements, the concept of successive trapping vacancies at group-V impurity atoms in irradiated n-Ge before and after $n \to p$ conversion may be adopted for irradiated n-Ge as an approach for consideration. Further theoretical calculations could be very useful for a fundamental understanding the problem.

The authors are greatly indebted to Professor G.D. Watkins for his interest to this work and his critical remarks while reading the manuscript. We also express our sincere gratitude to Professor A.R. Peaker and Dr. V.P. Markevich for our collaboration. Many useful discussions with Dr. Jose Coutinho and Dr. Alexandra Carvalho are highly appreciated.

References

[1] Gemanium-Based Technologies. From Materials to Devices, eds Cor Claeys and Eddy Simoen (Elsevier, Amsterdam–Boston–Heidelberg–London–New York–Oxford–Paris–San Diego–San Francisco–Singapore–Sydney–Tokyo, 2007).
[2] G.D. Watkins. Mater. Sci. Semicond. Processing, **3**, 227 (2000).
[3] V.V. Emtsev, T.V. Mashovets, S.M. Ryvkin. *Radiat. Damage and Def. in Semiconductors*. Inst. Phys. Conf. Ser. N 16 (The Institute of Physics, London and Bristol, 1972) p. 17.
[4] T.V. Mashovets, V.V. Emtsev. *Lattice Defects in Semiconductors, 1974*. Inst. Phys. Conf. Ser. N 23 (The Institute of Physics, London and Bristol, 1975) p. 103.
[5] V.V. Emtsev, T.V. Mashovets, E.A. Tropp. Fiz. Tekh. Poluprovodn., **12**, 293 (1978) (in Russian) [Engl. Transl. AIP: Sov. Phys. Semicond., **12** (2), 169 (1977)].
[6] J.S. Blakemore. *Semiconductor Statistics* (Pergamon Press, 1962).
[7] A.G. Abdusattarov, V.V. Emtsev, T.V. Mashovets. Sov. Tech. Phys. Lett. [(Engl. Transl. AIP), **12** (12), 606 (1986)].
[8] G.D. Watkins, J.W. Corbett. Phys. Rev., **134**, A1359 (1964).
[9] E.L. Elkin, G.D. Watkins. Phys. Rev., **174**, 881 (1968).
[10] R. Krause-Rehberg, H.S. Leipner. *Positron Annihilation in Semiconductors. Defect Studies*. Springer Series Solid-State Sciences, vol. **127** (Springer Verlag, Berlin–Heidelberg, 1999).
[11] N.Yu. Arutyunov, V.V. Emtsev. Mater. Sci. Semicond. Processing, **9**, 788 (2006).
[12] A. Nylandsted Larsen, A. Mesli. Physica B, **401–402**, 85 (2007).
[13] N.S. Patel', C. Monmeyran, A. Agarwal, L.C. Kimerling. J. Appl. Phys., **118**, 155702 (2015).
[14] J. Fage-Pedersen, A. Nylandsted Larsen, A. Mesli. Phys. Rev. B, **62**, 10116 (2000).
[15] V.P. Markevich, A.R. Peaker, V.V. Litvinov, V.V. Emtsev, L.I. Murin. J. Appl. Phys., **95**, 4078 (2004).
[16] V.P. Markevich, I.D. Hawkins, A.R. Peaker, K.V. Emtsev, V.V. Emtsev, V.V. Litvinov, L.I. Murin, L. Dobaczewski. Phys. Rev. B, **70**, 235213 (2004).
[17] V.P. Markevich. Mater. Sci. Semicond. Processing, **9**, 589 (2006).
[18] V.P. Markevich, A.R. Peaker, A.V. Markevich, V.V. Litvinov, L.I. Murin, V.V. Emtsev. Mater. Sci. Semicond. Processing, **9**, 613 (2006).
[19] A.V. Markevich, V.V. Litvinov, V.V. Emtsev, V.P. Markevich, A.R. Peaker. Physica B, **376–377**, 61 (2006).
[20] C. Nyamhere, F.D. Auret, A.G.M. Das, A. Chawanda. Physica B, **401–402**, 499 (2007).
[21] C.E. Lindberg, J. Lundsgaard Hansen, P. Bornholt, A. Mesli, K. Bonde Nielsen, A. Nylandsted Larsen, L. Dobaczewski. Appl. Phys. Letts, **87**, 172103 (2005).
[22] A. Nylandsted Larsen, A. Mesli, K.B. Nielsen, H. Kortegaard Nielsen, L. Dobaczewski, J. Adey, R. Jones, D.W. Palmer, P.R. Briddon, S. Öberg. Phys. Rev. Lett., **97**, 106402 (2006).
[23] G.D. Watkins, J.W. Corbett. Phys. Rev., **121**, 1001 (1961).
[24] P. Vanmeerbeek, P. Clauws. Phys. Rev. B, **64**, 245201 (2001).
[25] P. Vanmeerbeek, P. Clauws, H. Vrielinck, B. Pajot, L. Van Hoorebeke, A. Nylandsted Larsen. Phys. Rev. B, **70**, 035203 (2004).
[26] V.P. Markevich, I.D. Hawkins, A.R. Peaker, V.V. Litvinov, L.I. Murin, L. Dobaczewski, J.L. Lindström. Appl. Phys. Lett., **81**, 1821 (2002).
[27] V.P. Markevich, A.R. Peaker, A.V. Markevich, V.V. Litvinov, L.I. Murin, V.V. Emtsev. Mater. Sci. Semicond. Processing, **9**, 613 (2006).
[28] L.I. Khirunenko, Yu.V. Pomozov, M.G. Sosnin, N.V. Abrosimov, H. Riemann. AIP Conf. Proc., **1583**, 100 (2014).
[29] J. Coutinho, S. Öberg, V.J.B. Torres, M. Barroso, R. Jones, P.R. Briddon. Phys. Rev. B, **73**, 235213 (2006).
[30] J. Coutinho, V.J.B. Torres, A. Carvalho, R. Jones, S. Öberg, P.R. Briddon. Mater. Sci. Semicond. Processing, **9**, 477 (2006).
[31] A. Carvalho, R. Jones, J. Coutinho, M. Shaw, V.J.B. Torres, S. Öberg, P.R. Briddon. Mater. Sci. Semicond. Processing, **9**, 489 (2006).
[32] A. Carvalho, R. Jones, J. Coutinho, V.J.B. Torres, S. Öberg, J.M. Campanera Alsina, M. Shaw, P.R. Briddon. Phys. Rev. B, **75**, 115206 (2007).
[33] H. Höhler, N. Atodiresei, K. Schroeder, R. Zeller, P.H. Dederichs. Phys. Rev. B, **71**, 035212 (2005).
[34] A. Chroneos, R.W. Grimes, C. Tsamis. Mater. Sci. Semicond. Processing, **9**, 536 (2006).
[35] V.V. Emtsev, N.V. Abrosimov, V.V. Kozlovski, G.A. Oganesyan. Semiconductors (Pleiades Publishing Ltd.), **48**, 1438 (2014).

Редактор G.A. Oganesyan